

High-Resolution Low Latency and Low-Power Absolute Inductive Angle Encoder Reference Design



Description

This reference design demonstrates a high-resolution, absolute inductive angle encoder. A rotating conductive target printed circuit board (PCB) forms part of the design. The stationary PCB includes excitation and Nonius receiver coils as well as dual contactless inductive sensor front-ends with an inductor-capacitor (LC) oscillator and sine-cosine interfaces. An Arm® Cortex®-M0 microcontroller (MCU) with 4MSPS analog-to-digital converters (ADCs) calculates the absolute angle.

Resources

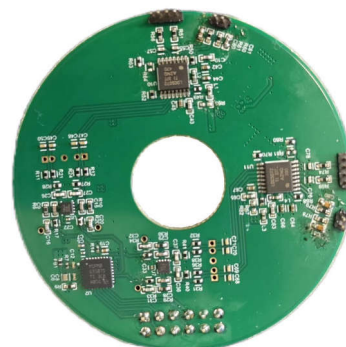
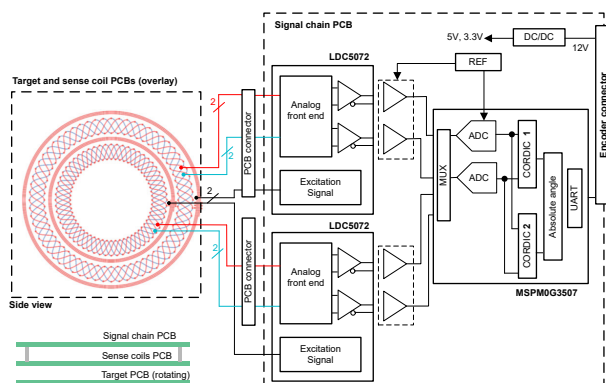
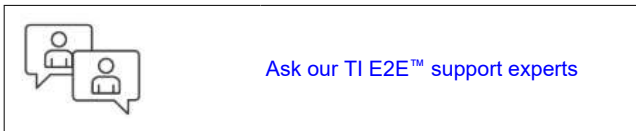
TIDA-010961	Design Folder
LDC5072, MSPM0G3507	Product Folder
TPSM365R3, REF3533	Product Folder
TLV9062	Product Folder

Features

- Absolute angle resolution 16.6 effective number of bits (ENOB), static angle accuracy $< 0.04^\circ$, very low latency 9.6 μ s
- 58mm diameter conductive target and sense PCB with two Nonius coils at 16 and 15 periods per turn enable a low-height design
- Immunity to stray magnetic fields enables resolver replacement at lower system cost, lower power consumption < 500 mW, and higher accuracy
- Integrated analog front-end IC for contactless inductive position sensing removes the need for magnets, lowering system cost
- MCU with integrated dual 12-bit Analog-to-Digital Converter (ADC), oversampling and trigonometric math accelerator help increase resolution and reduce system cost

Applications

- [Servo drive position sensor](#)
- [Robot position sensor](#)
- [Humanoid robot position sensor](#)
- [Traction inverter](#)



1 System Description

Single or multi-turn absolute rotary angle encoders support numerous applications including servo drives, industrial robots, and collaborative humanoid robots where precision mechanical angle positioning is required. The predominant types of position sensors are optical, magnetic, and inductive or capacitive. Large currents in nearby wiring necessitate advanced sensor technologies. One example is inductive sensors, which operate effectively in magnetic environments. Inductive sensors are immune to external stray fields and provide reliable measurements.

Figure 1-1 shows how this reference design demonstrates an absolute single-turn inductive rotary angle encoder. This inductive encoder is composed of three printed circuit boards (PCBs), the rotating target PCB, which is connected to the rotating motor shaft, and the stationary coil and signal chain PCBs.

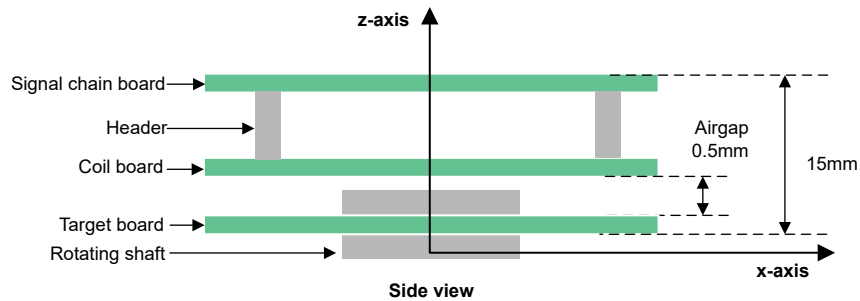


Figure 1-1. Inductive Angle Sensing Principle

The coil PCB contains two sets of exciter coils and receiver coils. The two sets of receiver coils implement 16 and 15 periods per turn to detect the absolute position at start-up, and offer a higher resolution compared to less periods per turn. The coil PCB connects to the signal chain PCB, which employs the dual LDC5072 inductive front ends and the MSPM0G3507 microcontroller. Figure 1-2 shows the rotating target PCB is a passive disc with conductive dual pattern printed on the PCB and a 58mm diameter.

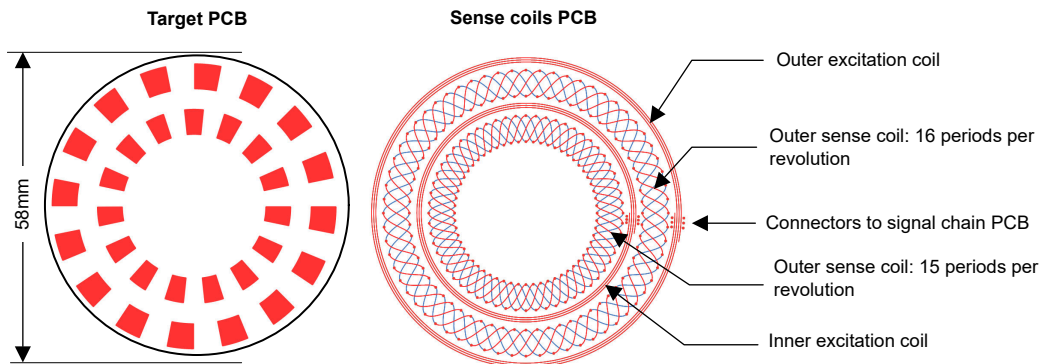


Figure 1-2. Target and Sense Coil PCB

Two LDC5072 inductive front-end ICs each produce high-frequency excitation signals. These signals are injected directly into corresponding exciter coils. The excitation coils generate a secondary voltage on the receiver coils depending on the rotary angle position of the target relative to the receiver coils. A signal representation of the position is obtained by reading in the voltages from the receiver coils. Each of the two LDC5072 devices process the signal, filter out the high-frequency excitation frequency, and provide an amplitude-modulated differential analog sine and cosine signal which tracks the electrical angle. The internal ADC of the MSPM0G3507 samples LDC5072 output signals at a 32kHz rate. The sensor performs initial gain and offset calibration on two signal tracks: one with 16 periods and the other with 15 periods. The sensor then detects rotary position start-up and calculates high-resolution absolute angles continuously.

1.1 Key System Specifications

Table 1-1 provides the key specifications of this reference design.

Table 1-1. TIDA-010961 Key Design Specifications

PARAMETER	VALUE (TYPICAL)	COMMENT
Function	Single-turn inductive absolute angle encoder	–
Inductive sensor type	LDC5072-Q1 inductive analog front end	–
Sense PCB coil outer diameter	58mm	–
Sense PCB coil shaft hole	16mm	–
Outer coil periods	16	–
Inner coil periods	15	–
Air gap between target and sense PCB	0.5mm (typical), 1.2mm (maximum)	Configurable, see definition in Figure 1-1
Angle accuracy	$\leq 0.04^\circ$	Offset and gain error calibrated at 25°C
Angle standard deviation (standard deviation)	$\leq 0.0015^\circ$	–
Angle resolution (ENOB)	16.6 effective number of bits (ENOB)	–
Angle resolution (numerical)	32-bit (IQ21)	Custom specific on MSPM0G3507
Angle propagation delay (latency)	9.6 μ s	Time from effective sampling point of inductive sense coil to angle calculated
Effective angle sample rate	32kHz	Configurable
Maximum operating speed	Not tested	Change low-pass filter cap to increase, see Section 3.1.3.1
A/D converter	Dual 12-bit ADC with 8-times oversampling decimation filter	Integrated to MSPM0G3507, ADC oversampling configurable up to 128 times
A/D converter oversampling rate	2.85MSPS (250ns sample time, 100ns conversion time)	Configurable sample time, 150ns minimum
Encoder connector	12-pin connector	See Table 4-2
Interface	UART	2.5M baud rate
Supply voltage	12V \pm 10%	–
Power consumption at 12V input	468 mW	–
Operating temperature range	–40°C to 125°C	Reference design tested at 25°C ambient temperature
Signal chain PCB layers	6	–

2 System Overview

2.1 Block Diagram

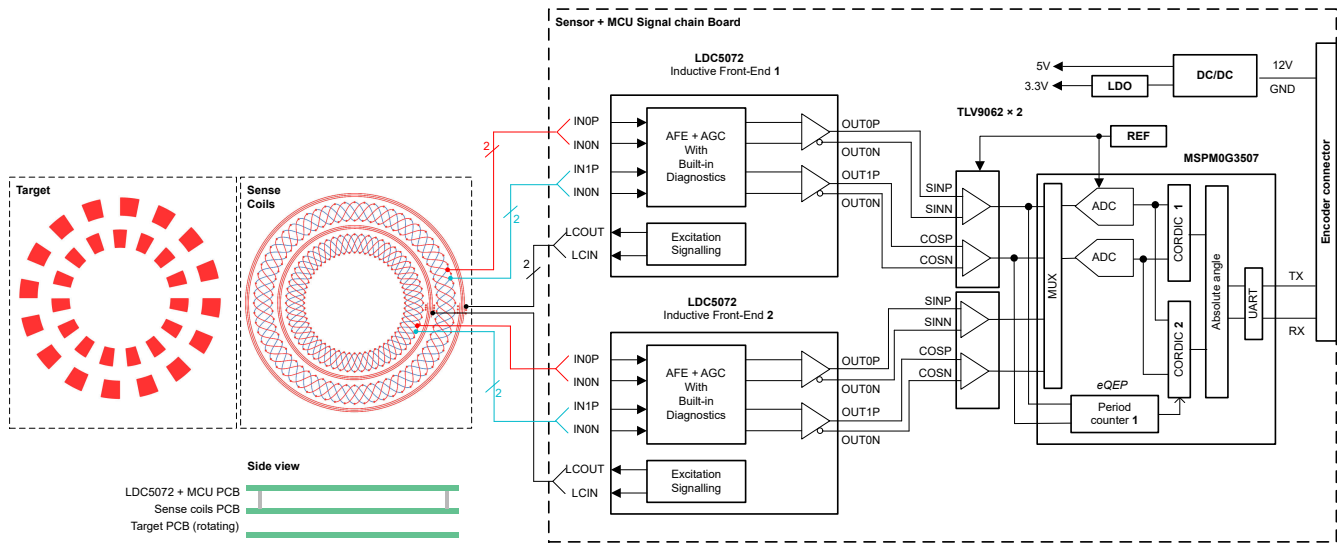


Figure 2-1. System Block Diagram

2.2 Design Considerations

Inductive encoders are an emerging trend in industrial position sensing applications due to the inherent immunity to external stray magnetic fields, low cost, and relatively high resolution. While mechanical resolvers are immune to external stray magnetic fields, PCB-based inductive angle sensors offer lower system cost, operate at lower power, offer higher accuracy, and built-in digital processing with a high EMC immunity bidirectional digital interface to the industrial drive.

Inductive sense technology typically requires a target board and a coil board. The conductive target board can be a pattern printed on a PCB, while the coil board contains both receiver and excitation coils. The coil PCB is stationary, while the target PCB is mounted to the motor shaft and rotates. The excitation coil generates a secondary voltage on the receiver coils depending on the position of the target relative to the receiver coils. A signal representation of the position is obtained by reading in and processing the voltages from the receiver coils, and giving analog outputs representing the sine and cosine components of the position of the target.

As [Figure 2-1](#) shows, the inductive encoder typically uses multipole pair receiver coils to get a higher resolution, but this indicator only provides incremental position. Nonius encoding is a method to get absolute position, Nonius encoding requires two sets of receiver coils with coprime periods.

The electrical signal chain offset and gain as well as sample rate, speed, and resolution of the ADC impact the angle accuracy. Components with very low temperature drift help reduce the angle error. Decoding of the angle from the sine and cosine sensor signals require math functions such as division, multiply-and-accumulate, and arctangent.

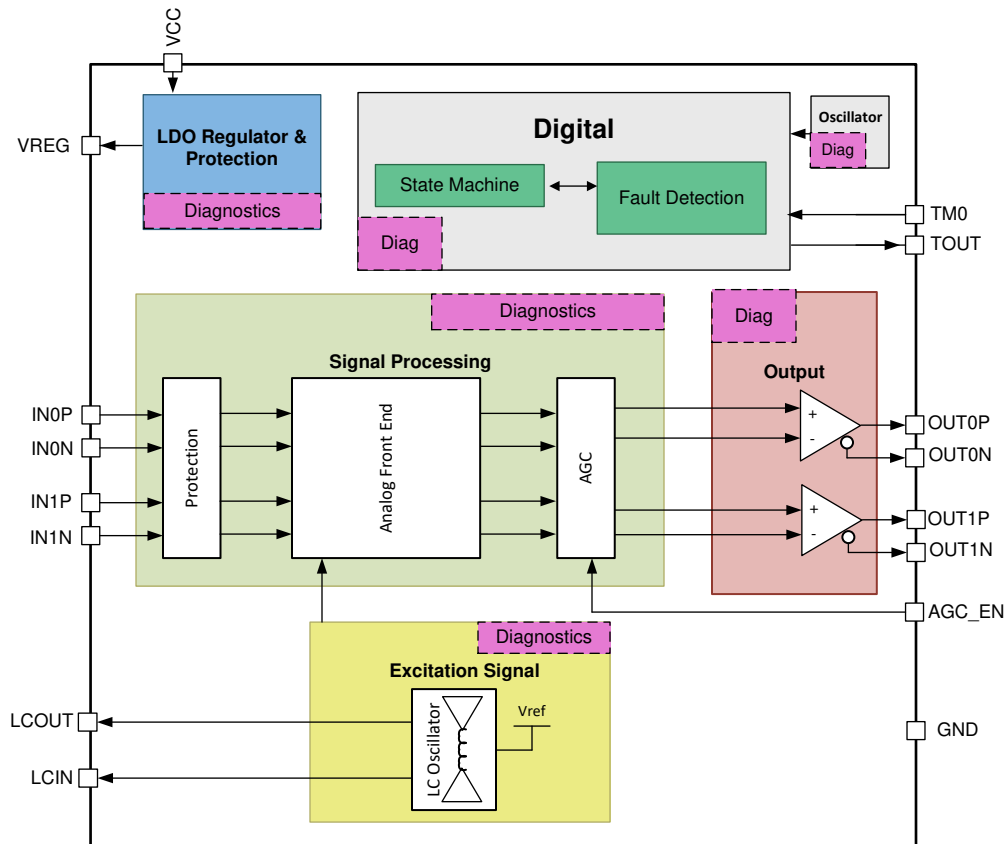
Small footprint circuits with high integration and low power consumption are critical to design the smallest form factor circular PCBs. Since the encoder can be motor integrated, ambient operating temperatures at least up to 125°C are typically required.

2.3 Highlighted Products

2.3.1 LDC5072-Q1

The LDC5072-Q1 IC is an analog front end for contactless, inductive position sensors targeted for absolute rotary position in automotive and industrial applications. The device features an integrated analog front end for contactless, inductive position sensors for absolute rotary position from 0° to 360°. The device is also equipped with numerous diagnostic features to detect, monitor, and report failures that either existed before the power-up or occurred during device operation. The key features with this design are:

- Integrated analog front-end IC for contactless, inductive position sensors for absolute rotary position from 0° to 360°
- Supports operation in harsh environments, immune to stray magnetic fields, dirt, and contamination
- Functional safety-compliant
- Temperature range -40°C to 160°C



Copyright © 2018, Texas Instruments Incorporated

Figure 2-2. LDC5072-Q1 Functional Block Diagram

2.3.2 MSPM0G3507

The MSPM0G350x microcontrollers (MCUs) are part of the MSP highly integrated, ultra-low-power 32-bit MCU family based on the enhanced Arm® Cortex®-M0+ 32-bit core platform operating at up to 80MHz frequency. These cost-optimized MCUs offer high-performance analog peripheral integration, support extended temperature ranges from -40°C to 125°C , and operate with supply voltages ranging from 1.62V to 3.6V. The MSPM0G350x MCU key features with this design are:

- Two simultaneous sampling 12-bit 4MSPS analog-to-digital converters (ADCs) with up to 17 external channels
- 14-bit effective resolution at 250kSPS with hardware averaging
- Math accelerator supports DIV, SQRT, MAC and TRIG computations
- Optimized low-power modes:
 - RUN: $96\mu\text{A}/\text{MHz}$ (CoreMark)
 - STANDBY: $1.5\mu\text{A}$ with real-time clock (RTC) and Static Random Access Memory (SRAM) retention

2.3.3 TPSM365R3

The TPSM365R3 is a 300mA, 65V input synchronous step-down DC/DC power module that combines power MOSFETs, integrated inductor, and boot capacitor in a compact QFN package. The key features with this device include:

- Integrated metal-oxide semiconductor field-effect transistors (MOSFETs), inductor, and controller in a $3.5\text{mm} \times 4.5\text{mm} \times 2\text{mm}$ QFN package
- Wide input voltage ranges from 3V to 65V
- Ultra-high efficiency $> 85\%$ across the full load range for minimum power dissipation ease motor integration
- Inherent protection features for robust design
- Extended industrial temperature range: -40°C to 125°C

2.3.4 TLV9062

The TLV9062 is a dual, low-voltage, (1.8V to 5.5V) operational amplifier (op amp) with rail-to-rail input- and output-swing capabilities. This device is a highly cost-effective design for applications where low-voltage operation, a small footprint, and high capacitive load drive are required. The key features with this device are:

- Rail-to-rail input and output
- Low input offset voltage: $\pm 0.3\text{mV}$
- Low broadband noise: $10\text{nV}/\sqrt{\text{Hz}}$
- Low input bias current: 0.5pA
- Unity-gain stable
- Internal Radio-Frequency Interference (RFI) and Electromagnetic Interference (EMI) filter

3 System Design Theory

3.1 Hardware Design

The hardware consists of three PCBs: (1) the rotating target PCB which connects to the motor shaft, (2) the stationary coil PCB, and the (3) signal chain PCB.

3.1.1 Target PCB

The target board is typically a patterned copper on a PCB. The periods of the pattern need to be same with period of the receiver coil on the coil board. This reference design uses 16 period and 15 period. The width and height of each pattern needs to match a single period of receiver coils.

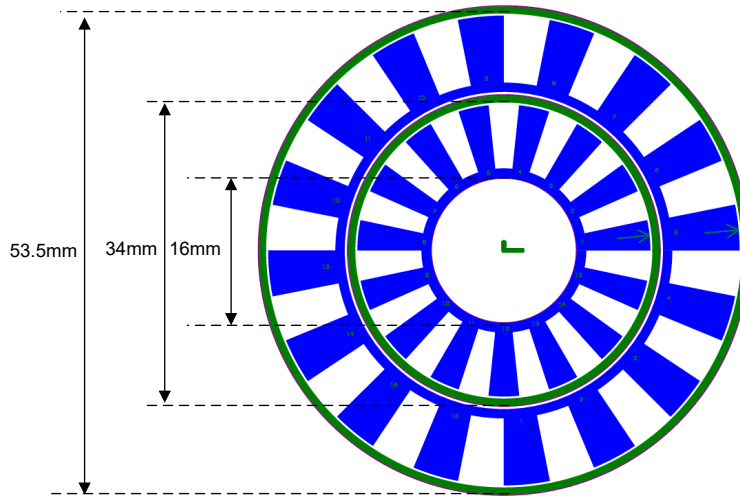


Figure 3-1. Target PCB

3.1.2 Coil PCB

The coil board contains the outer coils and inner coils. Each set of coils includes the excitation coils and receiver coils. Excitation coils have a spiral shape. Receiver coils have a sine or cosine shape.

The resolution of the inductive encoder mainly depends on the periods of coils. To get resolution higher than 16-bit ENOB, this reference design uses 16-periods outer coil and 15-periods inner coil. However, the PCB size also increases with higher periods of coils, the outer diameter of the coil is restricted to 58mm.

For the excitation coil, the inductance needs to be well controlled. The excitation coils perform as an inductor and are connected to the LCIN and LCOUT pins of the LDC5072 device. Two capacitors are also connected to these two pins which form the LC oscillator. The inductance and capacitance determine the excitation signal frequency. There is a balance between signal amplitude and power consumption. Higher signal amplitude means higher electromagnetic field which needs higher turns of excitation coils. To keep the inductance unchanged, the width of the coils needs to be reduced and leads to higher resistance and higher power consumption. This reference design controls the inductance of the excitation coils keeping around 5μH.

Both the excitation coil signal and receiver coil signal are high-frequency signals. To get better noise immunity, the reference design uses a six-layer PCB board and makes differential signal routing overlap in different layers.

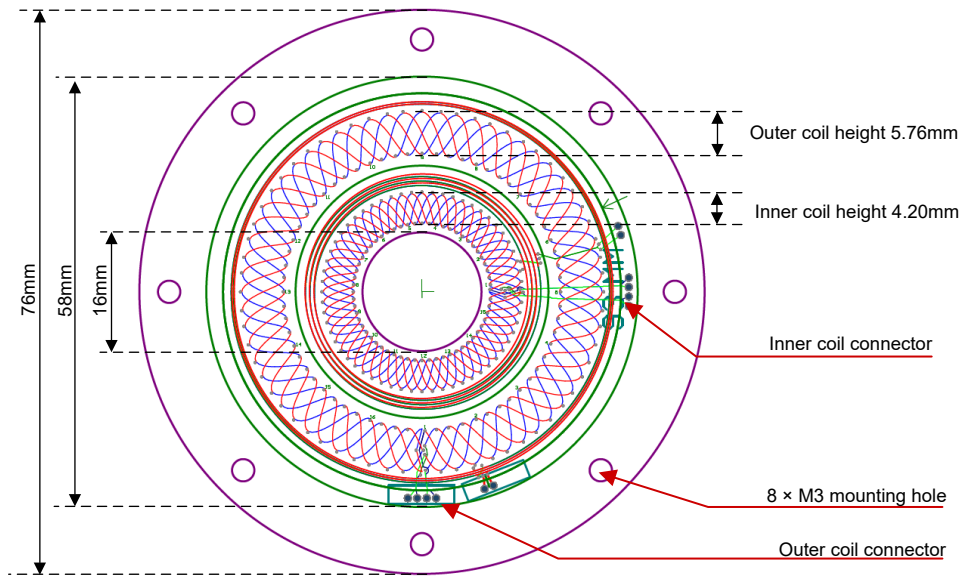


Figure 3-2. Coil PCB

3.1.3 Signal Chain PCB

3.1.3.1 Inductive Angle Position Sensor Front-End Schematic

Figure 3-3 shows the schematic of the inductive AFE for the outer sense coil. The comments apply to the schematic for the inner sense coil too.

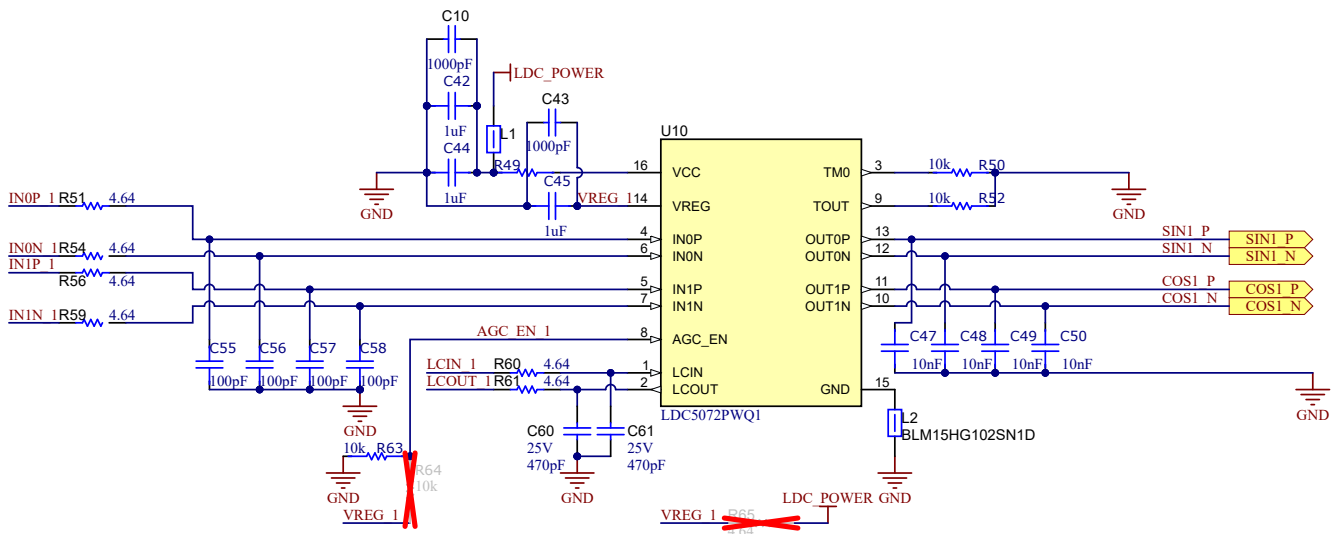


Figure 3-3. Inductive AFE LDC5072 Schematic

Three decoupling capacitors (C10, C42, and C44) are added close to LDC5072 VCC and the GND pin. C43 and C45 are decoupling capacitors placed close to VREG and the GND pin.

The LDC5072 device supports both 3.3V and 5V supply voltage at VCC. If 3.3V is supplied, both VCC and VREG are supplied from an external 3.3V power supply and R65 needs to be populated. If 5V is supplied, the LDC5072 uses an internal LDO to generate 3.3V for VREG and R65 needs to be removed.

The LDC5072 device supports both fixed-gain mode and automatic gain control (AGC) mode. R63 and R64 are resistor divider which control the gain setting. This reference design does not populate R64, making the LDC5072 device run in AGC mode.

C60, C61 (470pF), and the excitation coil on the sense coil PCB form the LC circuit. The outer excitation inductance (L) of the coil is design as 5μH, so the resonant frequency of the LC circuit is 4.6MHz and can be calculated in formula:

$$f_{osc} = \frac{1}{2\pi\sqrt{L\frac{C_{60}C_{61}}{C_{60} + C_{61}}}} \tag{1}$$

R51, C55, R54, C56, R56, C57 and R59, and C58 implement the low-pass filter for the sensor coil sine and cosine output.

C47, C48, C49, and C50 are 10nF and form a low-pass filter with the LDC5072 output impedance. For higher speeds, reduce the capacitors and see the data sheet for selection of the capacitor.

3.1.3.2 Differential to Single-Ended Signal Conversion

The TLV9062 is used to implement a differential-ended to single-ended circuit to drive the single-ended ADC in the MSPM0 MCU. The differential gain of TLV9062 is set to 0.5 and the bias voltage is set to 1.65V with a 3.3V voltage reference (REF3533) to get a unipolar signal from 0V–3.3V.

The bandwidth is configured for around 1MHz, less than half of the 2.8MSPS ADC sample rate. The first filter with the TLV9062 is set to 1.6MHz with C9 (20pF) and C24, C26 (10pF each), the second filter R17 (500) and C16 (200pF) is set to 1.6MHz.

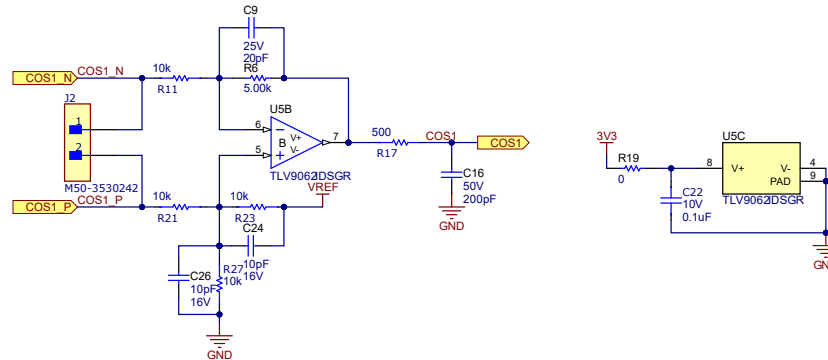


Figure 3-4. TLV9062 Schematic

3.1.4 MSPM0G3507 Schematic Design

The ceramic decoupling capacitors C3(10μF) and C4(1μF) are placed across the VDD and VSS pins, and C1(100nF), C2(0.47μF) are placed across the VCORE and VSS pins. A ferrite bead FB1 is added between VDD and the 3.3V power rail to avoid the high-frequency digital current populating the analog signal.

The NRST reset pin is pulled up to VDD with a 47kΩ resistor (R2) and 10nF pulldown capacitor (C7). The SYSOSC frequency correction loop (FCL) circuit utilizes an external 100kΩ with 0.1% tolerance resistor R5 populated between the ROSC pin and VSS.

MSPM0 accepts external ADC reference to improve ADC ENOB. In TIDA-010961, REF3533 is used as external reference and whose outputs are connected to the VREF+ and VREF– pins of M0. The C10(100nF) decoupling capacitor is placed across VREF+ and VREF–.

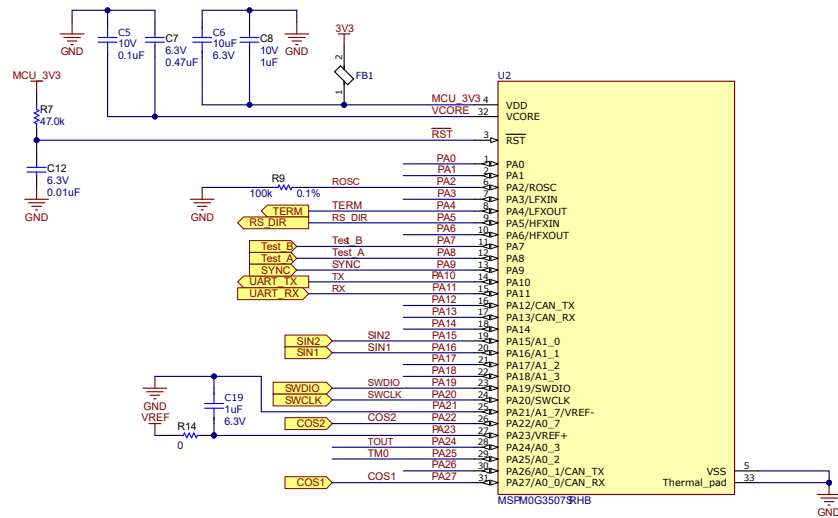


Figure 3-5. MSPM0G3507 Schematic

3.1.5 Power Supply Design

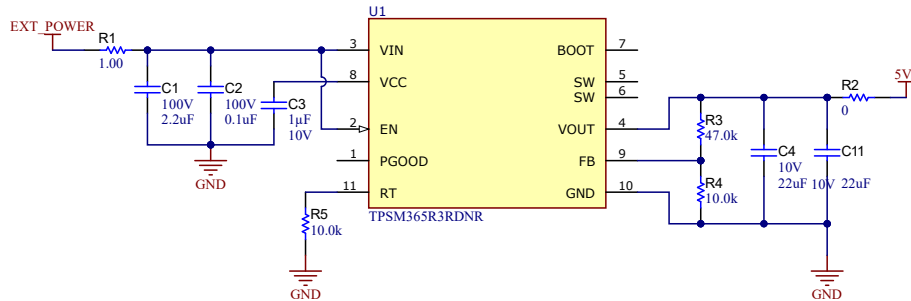


Figure 3-6. Input Power Supply Schematic

The nominal input supply voltage is 24V with a maximum input voltage range of 60V. The TPSM365R3 DCDC buck module accepts up to 65V input and generates a 5.5V intermediate power rail. C1, C2, and C3 are decoupling capacitors and are placed close to VIN and the GND PIN. R5 configures the switching frequency of this converter, the 10kΩ resistor is set to 1500kHz. R3 and R4 set the output voltage to 5.5V. Equation 2 shows that the output voltage can be calculated with $V_{FB} = 1V$.

$$V_{out} = V_{FB} \frac{R_4 + R_3}{R_4} \quad (2)$$

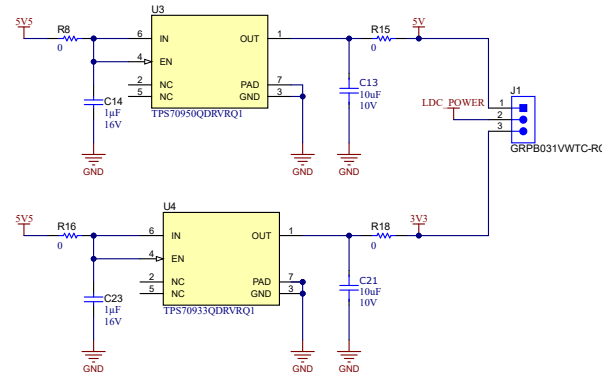


Figure 3-7. 5V and 3.3V Point-of-Load Supply Schematic

The LDO TPS70950 generates 5V from the intermediate 5.5V input for LDC5072. The LDO TPS70933 generates a 3.3V rail for LDC5072, TLV9062, and MSPM0G3507. The J1 jumper selects the LDC5072 supply voltage, either 3.3V or 5V. The 1µF capacitors C14 and C23 are added for noise decoupling and 10µF output capacitors C13 and C21 are added for stable operation.

The voltage reference REF3533 is powered by the 5V supply and generates precise 3.3V output as the reference of the MSPM0 ADC. Similarly, with the TPS7A0533, C8 (100nF) is needed for decoupling and C9 (1µF) are used for stable operation.

3.2 Absolute Position Calculation

To get absolute position, this reference design uses dual track coils with coprime periods. The outer side track uses 16 periods coils while the inner track uses 15 periods coils.

To better illustrate how to calculate the absolute position, the design guide takes the outer coil with four periods and the inner coil with three periods, for example.

Figure 3-8 illustrates the relationship between the electrical angle of the outer coils and inner coils over one mechanical revolution with a lower period count of four and three for simplicity.

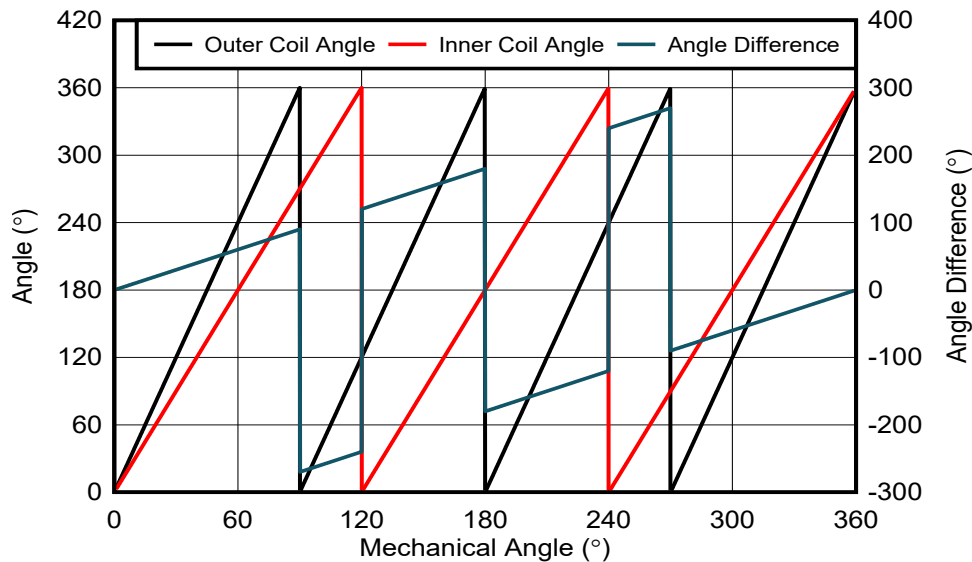


Figure 3-8. Outer and Inner Coil Angle Relationship With Coprime Four and Three Periods

The absolute mechanical angle is determined by the electrical angle difference between the coprime coils in the example 4 and 3.

Table 3-1. Relationship Between Electrical Angle Difference and Absolute Angle

DIFFERENCE ANGLE (°)	ABSOLUTE ANGLE (°)
0 to 90	N4 ⁽¹⁾
-270 to -240	90 + N4 ⁽¹⁾
120 to 180	90 + N4 ⁽¹⁾
-180 to 120	180 + N4 ⁽¹⁾
240 to 270	180 + N4 ⁽¹⁾
-90 to 0	270 + N4 ⁽¹⁾

(1) N4 means the outer coils mechanical angle.

In this reference design, coprime 16 and 15 coils are used. The 16 periods coils divide the absolute angle into 16 sectors. Assuming the absolute angle falls within n^{th} sector, the outer coils angle are either $n \times 22.5^\circ$ greater than or $360 - n \times 22.5^\circ$ less than the inner coils angle. Equation 3 calculates the sector number.

$$\text{sector} = \begin{cases} \text{FLOOR}\left(\frac{\text{outer coil angle} - \text{inner coil angle}}{22.5}\right) & \text{outer coil angle} \geq \text{inner coil angle} \\ \text{FLOOR}\left(\frac{\text{outer coil angle} - \text{inner coil angle} + 360}{22.5}\right) & \text{outer coil angle} < \text{inner coil angle} \end{cases} \quad (3)$$

Then, the absolute angle can be calculated as:

$$\text{absolute position} = \text{sector} \times 22.5^\circ + \text{fine angle}/16 \quad (4)$$

Figure 3-9 shows the absolute position calculation flow chart in a Nonius encoder.

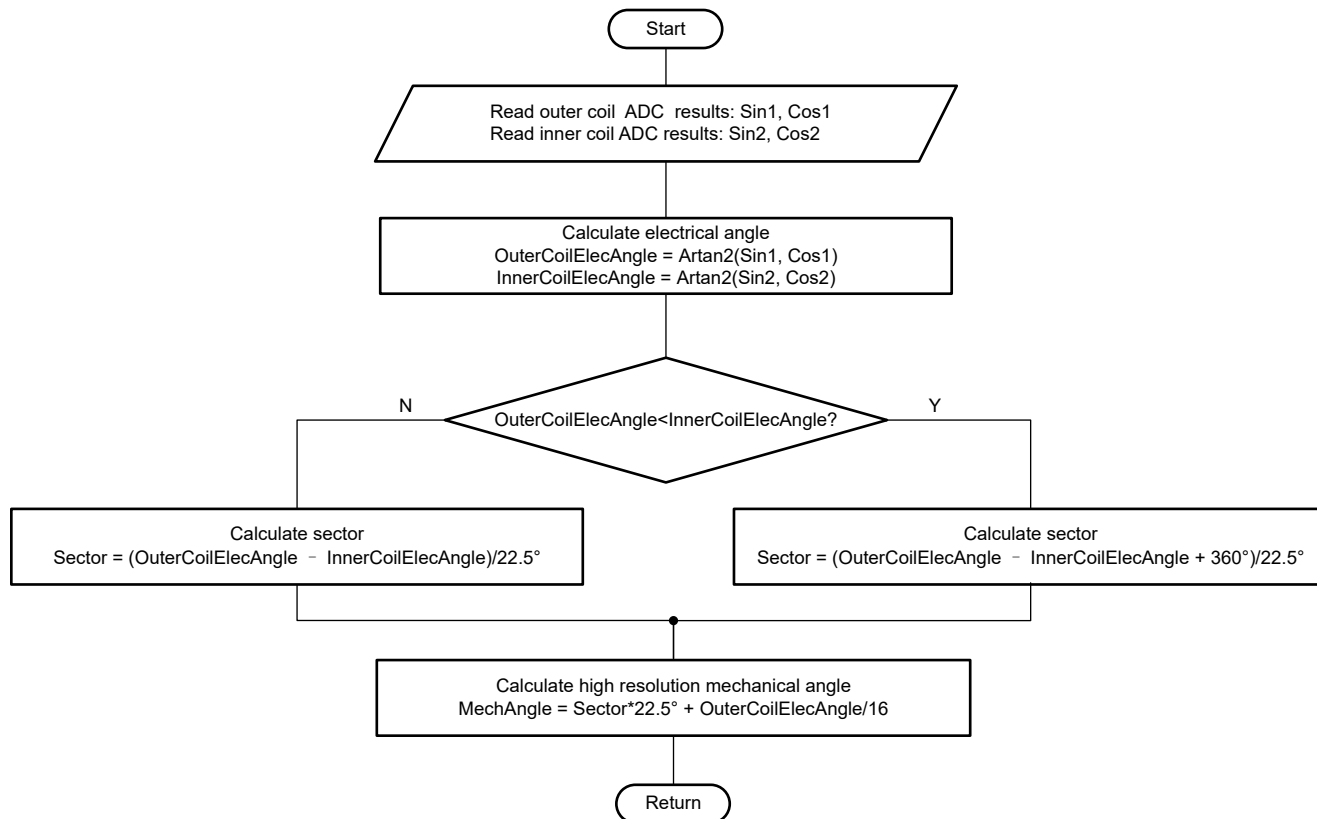


Figure 3-9. Rotary Angle Calculation Flow Chart

3.3 Software Design

An internal TI test software validates this reference design with the MSPM0G3507 using the MSPM0 software development kit for M0 MCUs.

3.3.1 Angle Calculation Timing

In the TIDA-010961 reference design, the MSPM0G3507 samples the output sine signals and cosine signals of the LDC5072 device with 8 × oversampling ratio and calculates the absolute angle. The ADC in the TMAG6180 device is triggered by an internal 32kHz Timer0 and saves the ADC results to arrays. After the ADC finishes the transaction, an interrupt is created, in which the MCU calculates the absolute angle.

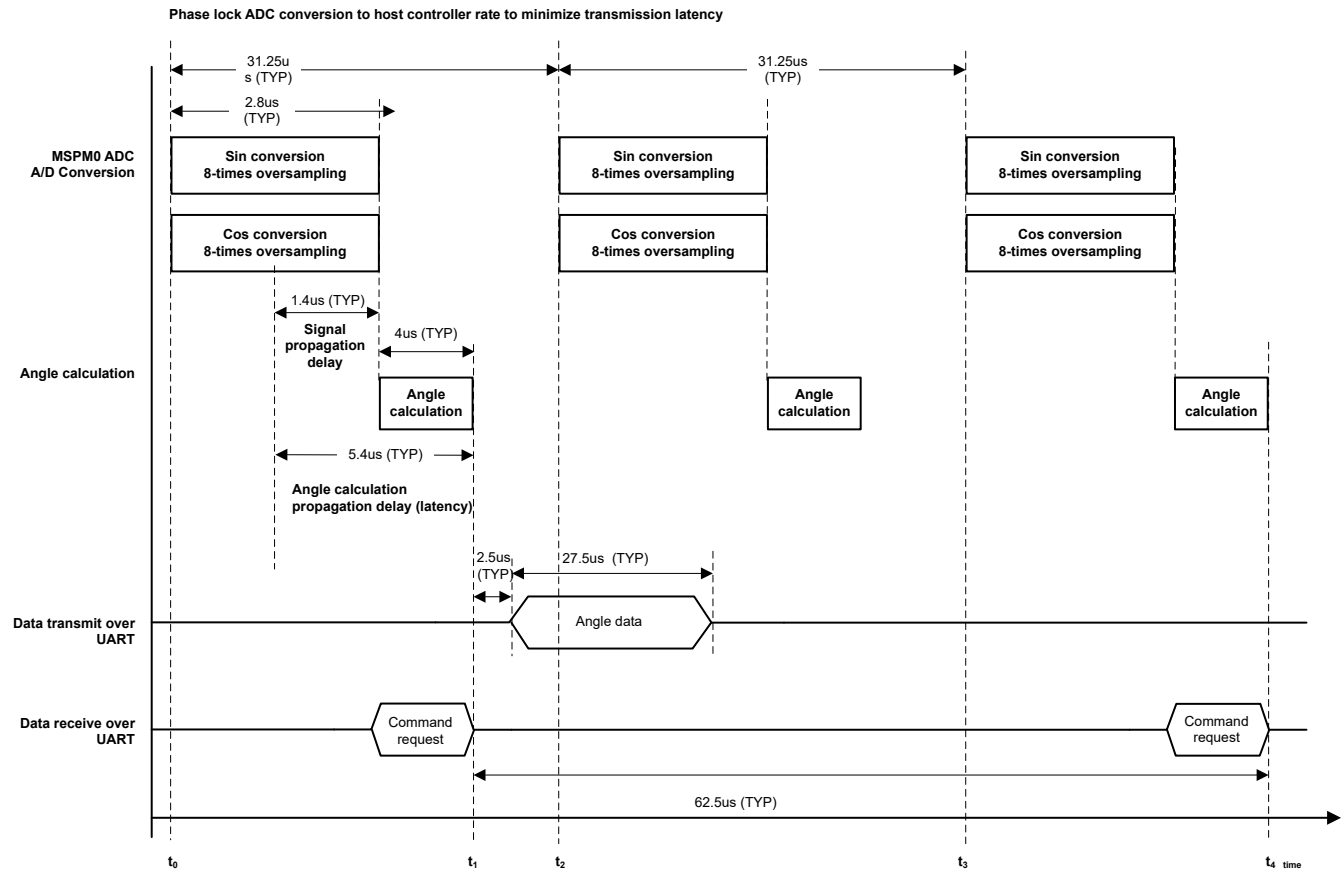


Figure 3-10. MSPM0G3507 Timing Diagram

The host controller sends command requests to get position data from the TIDA-010961. The command triggers the UART interrupt in MSPM0, then the MCU sends the position data.

Table 3-2. System Latency Analysis

SUBSYSTEM	PROPAGATION DELAY (TYPICAL)
LVD5072	4µs
Differential to single-ended filter	0.2µs
8 times oversampling ADC	1.4µs
Angle calculation	4µs
Total	9.6µs

3.3.2 Rotary Angle Error Sources and Compensation

Align the center of the target board to the center of the coil board, with acceptable tolerances, for accurate angle measurement. Follow these steps to calibrate the encoder for best accuracy:

- Set the reference angle based on the magnet alignment to the sensor. This error can be saved in the microcontroller for runtime absolute position calculation. This error is also known as Angle offset in a system.
- Electrical offset calibration - See the [Calibration of AMR Angle Sensors](#) application report for the offset calibration procedure. If the sensor cannot be rotated across the full range, then the electrical offsets cannot be calibrated.
- Amplitude mismatch calibration - See the [Calibration of AMR Angle Sensors](#) application report for the amplitude mismatch calibration procedure. If the sensor cannot be rotated across the full range, then the amplitude mismatch cannot be calibrated.

Further error sources include nonlinearity of the sensor signal chain such as the 3rd harmonics, and a mechanical error through coupling a reference angle encoder to the shaft of the absolute inductive encoder.

The following figures outline the error source and the impact to the angular error to understand and compensate these types of errors.

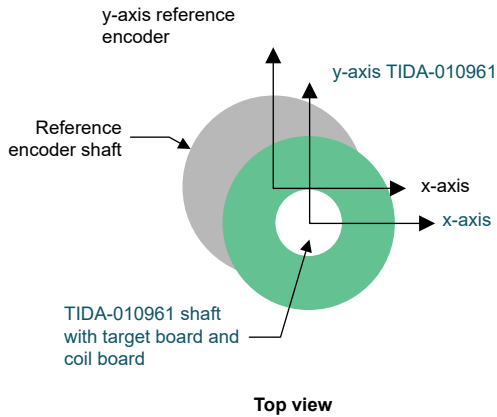


Figure 3-11. Shaft Adapter Mechanical Displacement

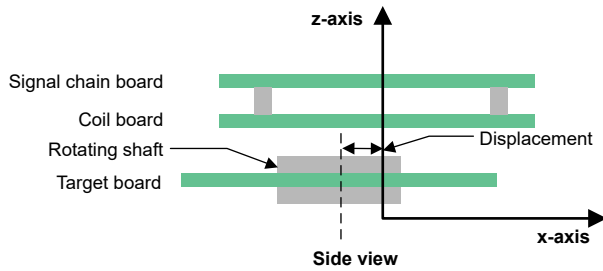


Figure 3-13. Target Board and Coil Board Displacement

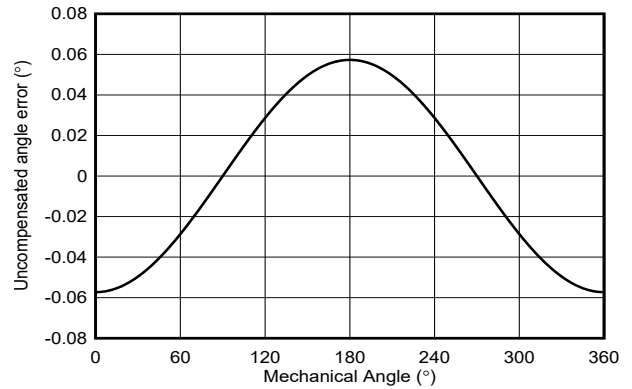


Figure 3-12. Mechanical Angle Error Due to Shaft Adapter Displacement

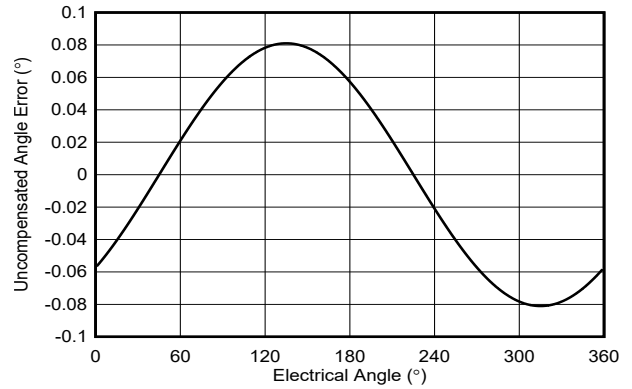


Figure 3-14. Electrical Angle Error due to Target Board and Coil Board Displacement

Figure 3-15 to Figure 3-17 show examples of the electrical offset, gain-mismatch and nonlinearity (3rd harmonics) of the sensor signal chain impact the angle error.

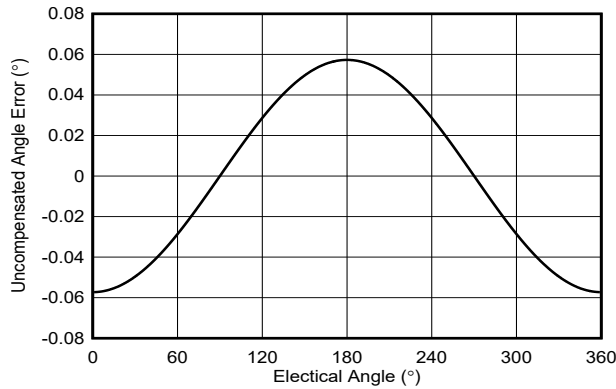


Figure 3-15. Electrical Angle Error due to Sine Signal and Cosine Signal Chain Offset (0.1%)

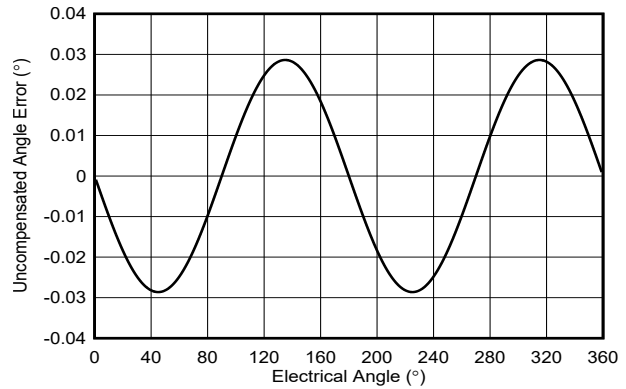


Figure 3-16. Electrical Angle Error due to Sine Signal and Cosine Signal Gain Mismatch (0.1%)

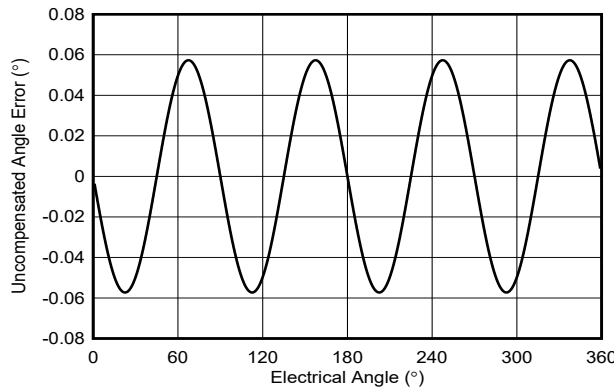


Figure 3-17. Electrical Angle Error due to Sine Signal and Cosine Signal Chain Nonlinearity (0.1%)

Because the outer coils have 16 periods, multiply the *electrical* angle error order by 16 to get the *mechanical* angle error order. Table 3-3 summarizes the impact on the angular error pattern.

Table 3-3. Errors Sources and Impact on Angle Error Harmonics

ERROR SOURCES	SHAFT COUPLING DISPLACEMENT	TARGET BOARD AND COIL BOARD DISPLACEMENT	SIGNAL CHAIN OFFSET	SIGNAL CHAIN GAIN MISMATCH	SIGNAL CHAIN NONLINEARITY (3 RD HARMONIC)
ELECTRICAL ANGULAR ERROR HARMONIC	–	1st	1st	2nd	4th
MECHANICAL ANGULAR ERROR HARMONIC	1st	16th	16th	32nd	64th

For more information on angle position calculation algorithms, see also the [Achieving Highest System Angle Sensing Accuracy](#) application report.

4 Hardware, Software, Testing Requirements, and Test Results

4.1 Hardware Requirements

The hardware equipment listed in [Table 4-1](#) is used to evaluate this reference design.

Table 4-1. Hardware Prerequisites

EQUIPMENT	COMMENT
TIDA-010961	This reference design
LBY80-C	2D linear stage
TIDA-010956	48V, 85A three-phase inverter reference design for integrated motor drives
MS1H4-40B30CA	Servo motor with 23-bit optical encoder

4.1.1 PCB Overview

[Figure 4-1](#) and [Figure 4-2](#) show the PCB top and bottom views.

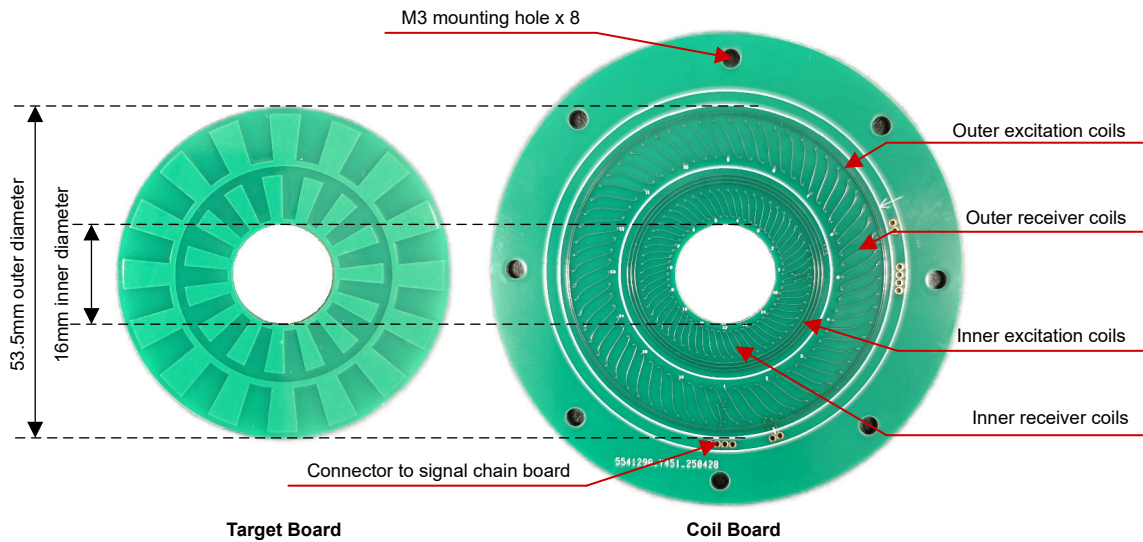


Figure 4-1. Target PCB (Left) and Sense Coil PCB (Right)

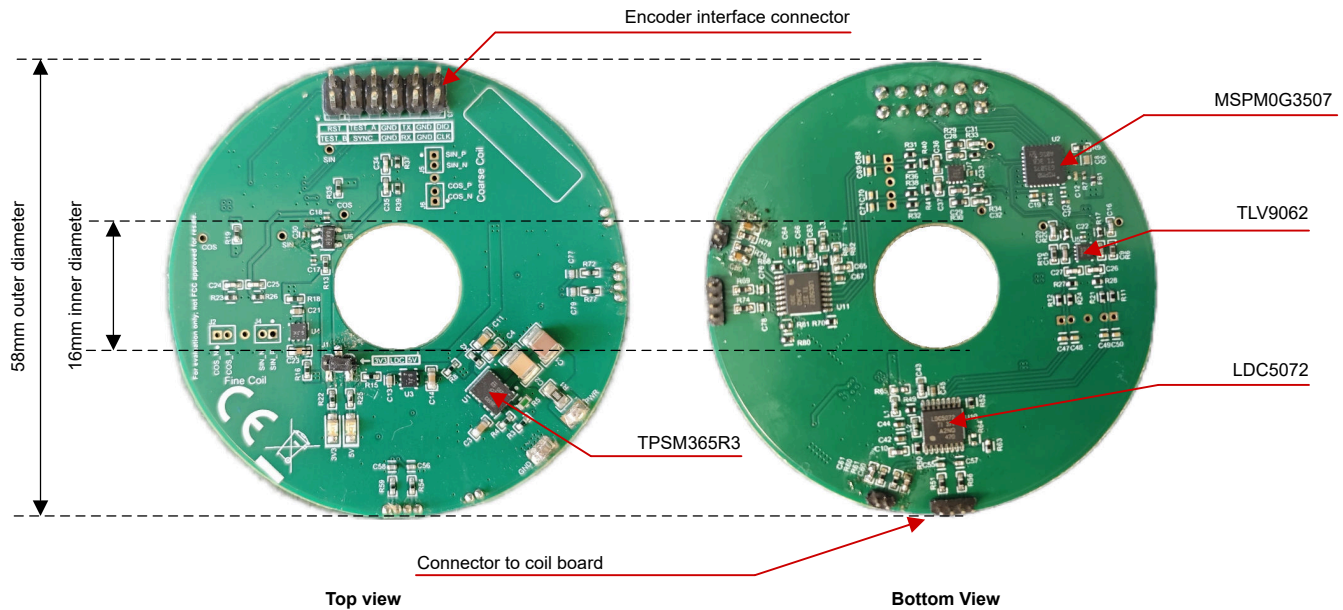


Figure 4-2. Signal Chain Board Top View (Left) and Bottom View (Right)

4.1.2 Encoder Interface

Table 4-2 shows the TIDA-010961 interface J3. The table includes UART and the JTAG interface. The UART is used to communicate the angle with the host MCU. JTAG is used to download and debug the software. The interface leaves some test pins for debugging.

Table 4-2. Interface Specification Header

PIN	SIGNAL	I/O	PIN	SIGNAL	I/O
J3-1	TEST_A	O	J3-2	RST	I
J3-3	SYNC	I	J3-4	TEST_A	O
J3-5	GND	–	J3-6	GND	–
J3-7	UART RX	I	J3-8	UART TX	O
J3-9	GND	–	J3-10	GND	–
J3-11	CLK	I	J3-12	DIO	I/O

4.2 Software

An internal TI test software validates this reference design with the MSPM0G3507 using the MSPM0 software development kit for M0 MCUs.

Table 4-3 lists the key software configuration.

Table 4-3. Software Configuration

SUBSYSTEM	PARAMETER	VALUE
Interrupt	ADC trigger frequency	32kHz
	Position calculation frequency	32kHz
ADC	Hardware oversampling ratio (OSR)	8
	Sampling time	280ns
UART	Baud rate	2.5M
	Word length	8bit

4.3 Test Setup

Figure 4-3 shows the encoder test bench.

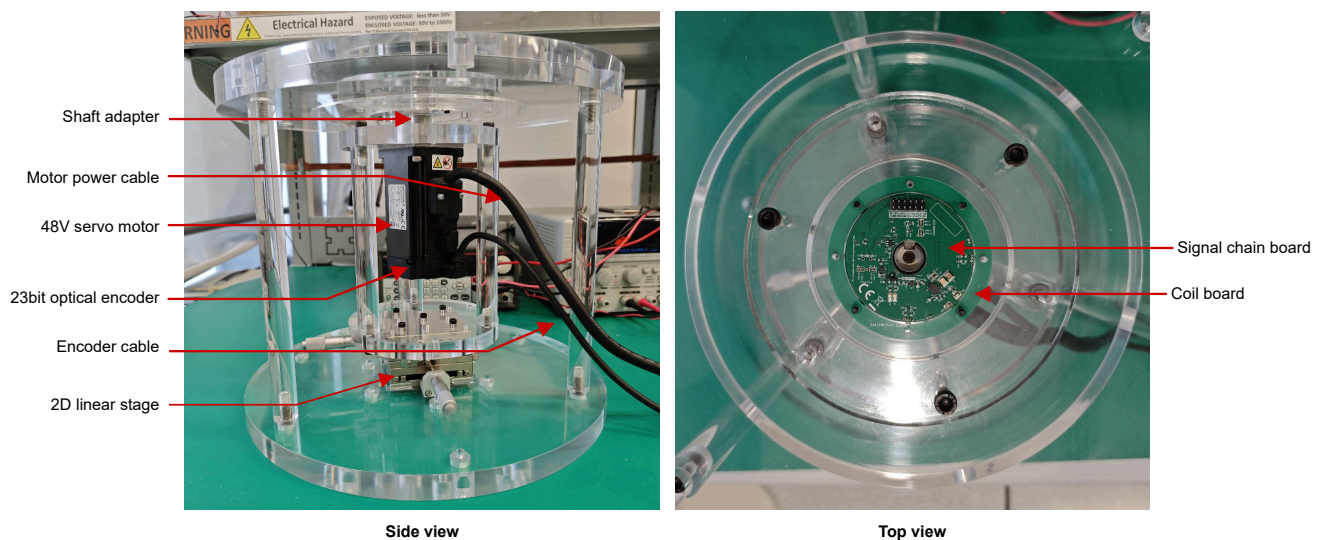


Figure 4-3. Encoder Test Bench

Figure 4-3 shows the whole test setup. MS1H4-40B30CA is a 48V servo motor with 23-bit optical encoder inside. The high-resolution optical encoder provides an accurate reference position to calculate the position measurement error.

The 2D linear stage is used to adjust the XY position of the receiver board, so that target board and receiver board can be precisely center aligned.

The TIDA-010956 three-phase inverter runs the motor at constant speed. The test bench uses a TMS320F280039 real-time MCU LaunchPad™ development kit to control the three-phase inverter and send position request commands to the reference encoder and TIDA-010961 simultaneously.

4.4 Test Results

4.4.1 Inductive Sensor Sine and Cosine Noise Measurement

Figure 4-4 and Figure 4-5 show the measured sine and cosine signals of the outer coil with 16 periods at the 7th sector over one electrical period. This corresponds to a mechanical angle from 135 degrees to 157.5 degrees. The maximum and minimum voltage of the sine is 3.036V and 0.123V. The cosine signal range is 3.176V and 0.232V. There is gain and an offset mismatch between the sine and cosine signals, which causes 1st harmonic electrical angle error. Minimize this error with calibration.

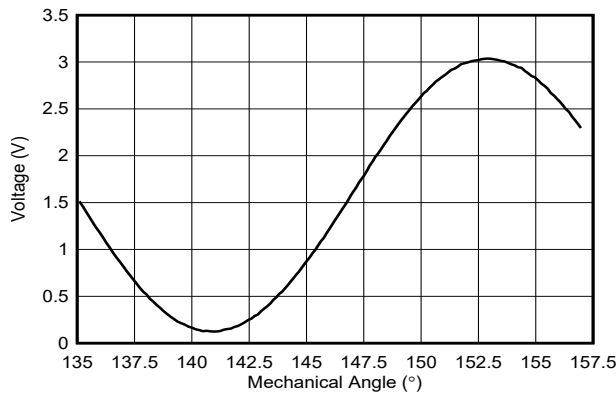


Figure 4-4. Sine Over One Electrical Cycle

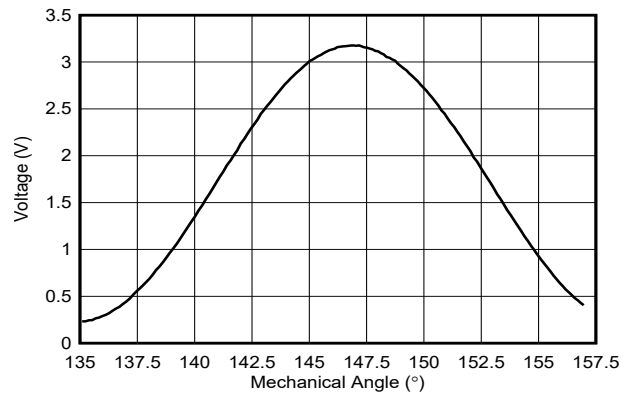


Figure 4-5. Cosine Over One Electrical Cycle

The following figures show the sine and cosine signal noise and histogram plots at a fixed 0.5 degrees mechanical angle. For the analysis, 2000 samples of the sine and cosine signals of the outer and inner loop were conducted at a sample rate of 32kHz with 8 × oversampling.

Table 4-4 shows the standard deviation, signal-to-noise ratio (SNR), and effective number of bits (ENOB) versus full-scale range. The absolute angle position data is calculated by the outer coil after the absolute angle is detected at start-up, the inner coil noise does not influence the final accuracy.

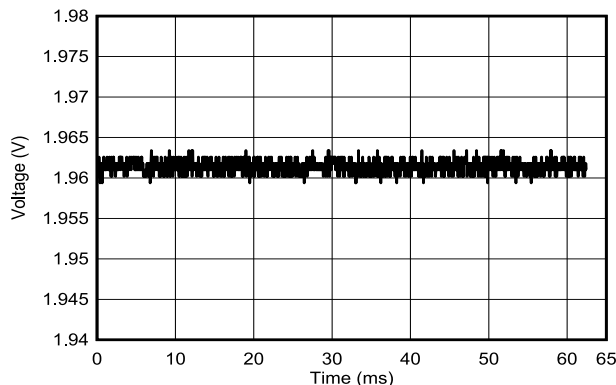


Figure 4-6. Outer Coil Sine Signal at 0.5 Degrees

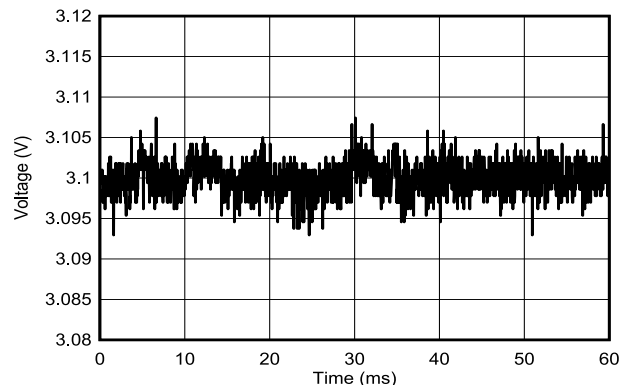


Figure 4-7. Outer Coil Cosine Signal at 0.5 Degrees

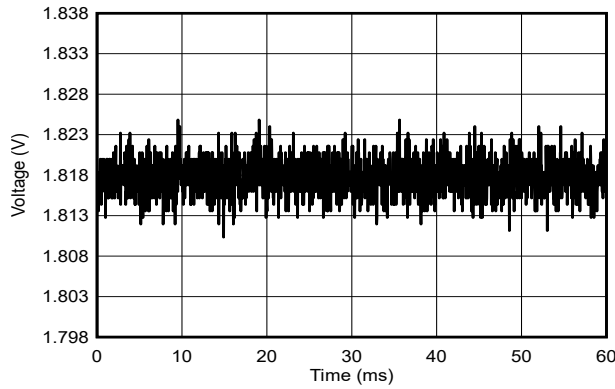


Figure 4-8. Inner Coil Sine Signal at 0.5 Degrees

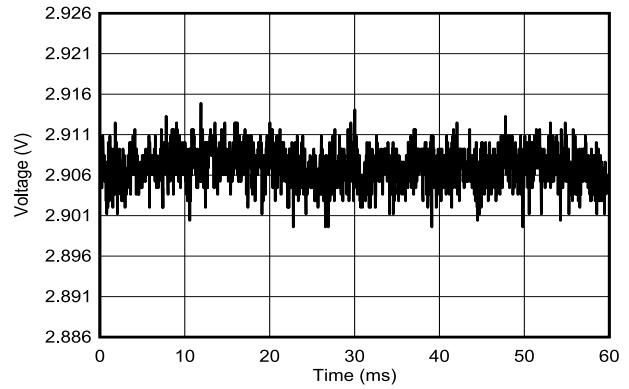


Figure 4-9. Inner Coil Cosine Signal at 0.5 Degrees

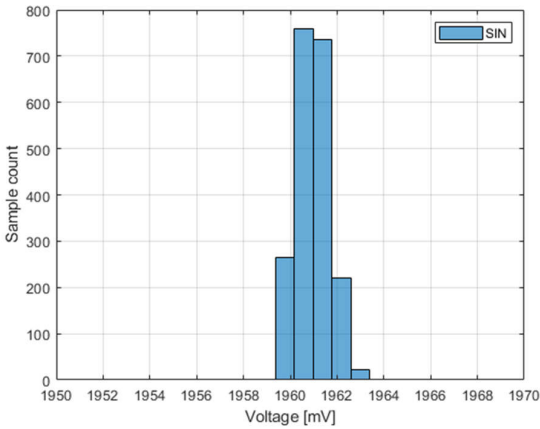


Figure 4-10. Histogram Outer Coil Sine

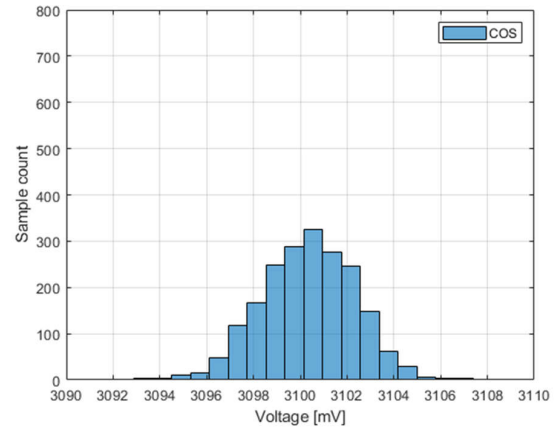


Figure 4-11. Histogram Outer Coil Cosine

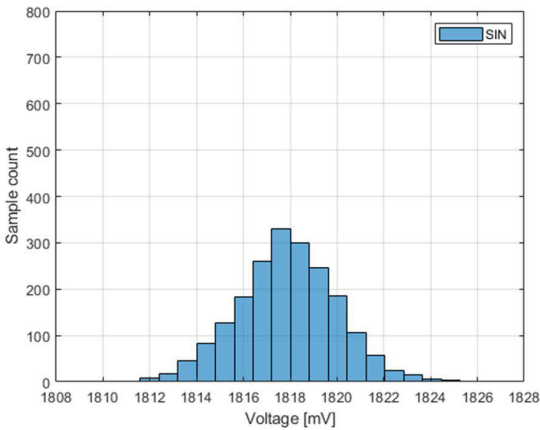


Figure 4-12. Histogram Inner Coil Sine

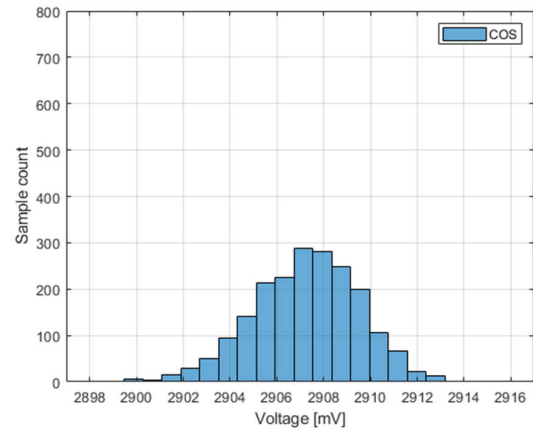


Figure 4-13. Histogram Inner Coil Cosine

Table 4-4. Standard Deviation, SNR and ENOB versus MSPM0 ADC Full-Scale Range

PARAMETER	OUTER COIL SINE	OUTER COIL COSINE	INNER COIL SINE	INNER COIL COSINE
Sine/Cosine amplitude (V)	1.45			
Standard deviation (mV)	0.73	2.00	2.13	2.24
SNR (dB)	66.0	57.2	56.7	56.2
ENOB (bit)	10.66	9.21	9.12	9.05

4.4.2 Absolute Angle Noise Measurement

For this test, the mechanical angle is fixed at 5.1 degrees. The angle is read at a 16kHz sample rate. For the analysis, 2000 samples are taken. Figure 4-14 and Figure 4-15 show the time domain noise and the histogram, respectively.

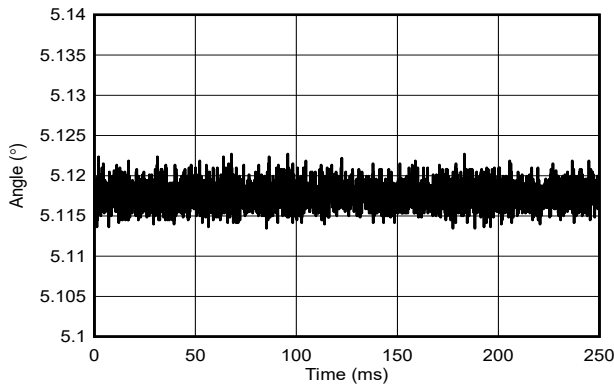


Figure 4-14. Static Angle at 5.1 Degrees Over 2000 Samples at 16kHz Sample Rate

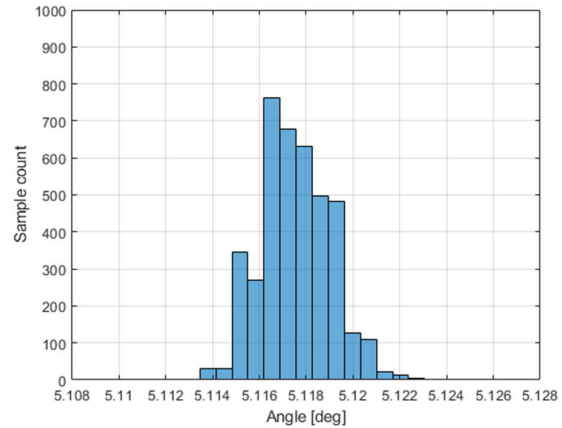


Figure 4-15. Histogram of the Angle at 5.1 Degrees

Table 4-5 shows the corresponding standard deviation and ENOB versus full-scale position measurement range.

Table 4-5. Standard Deviation, SNR and ENOB at Static Mechanical Angle of 5.1 Degrees

PARAMETER	ABSOLUTE ANGLE	COMMENT
Standard deviation (degree)	0.0015	RMS
SNR (dB)	101.6	$SNR = 20 \times \log_{10} (\pm 180 \text{ deg} / \text{STDEV})$
ENOB (bit)	16.6	$ENOB = (SNR - 1.76) / 6.02$

For the following test the angle is changed at a 22.5 degrees interval to validate the noise floor over all 16 electrical periods, which equals one turn. There is no significant difference in each of the eight electrical periods. The peak-to-peak static angle noise is around 0.02 degrees and a maximum value occurs at 225 degrees.

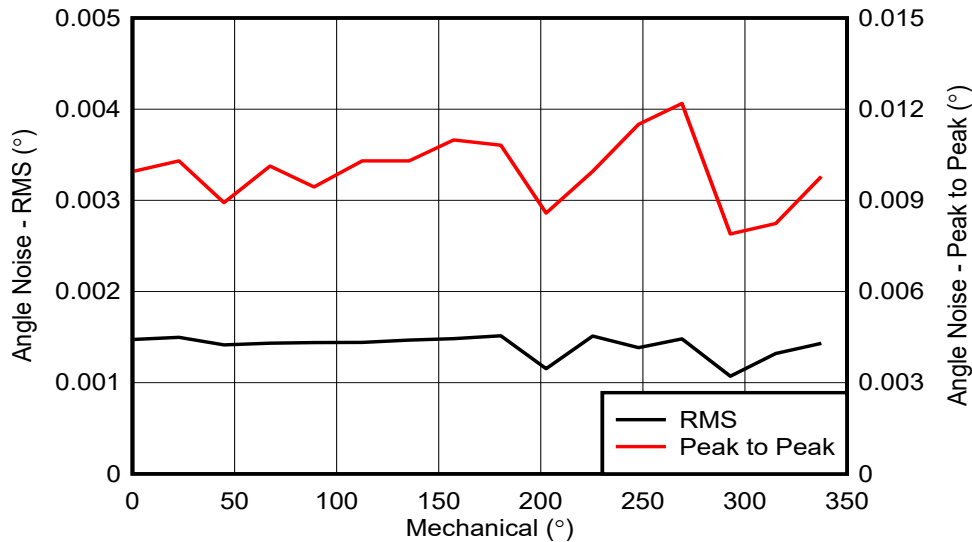


Figure 4-16. Static Angle Noise Over One Revolution

The following test is conducted to validate the static noise versus the air gap.

With the air gap increasing, the eddy current generated in the target board decreases and the output signal amplitude in the receiver coils also decreases, so the angle noise also becomes higher which means the encoder resolution is lower. When the air gap is increased to 1.5mm, the LDC5072 device on the inner coil runs into fault mode because the signal of the receiver coil is very small. Therefore, the absolute position cannot be calculated, keep the air gap smaller than 1.5mm.

Table 4-6. Angle Noise of Outer Coil versus Air Gap

Air Gap (mm) ⁽¹⁾	0.5 (Default)	0.8	1.2	1.5
Static Angle Noise (1 Sigma) (deg)	0.0015	0.0023	0.0025	0.0048

(1) The air gap is the distance between top of target board and bottom of coil board.

4.4.3 Rotary Angle Accuracy Measurement

In this section, the angle accuracy is tested when the motor is running at a constant speed of 30rpm. The host controller sends a position data request command at 16kHz frequency and collects the reference encoder and the synchronized position data time of the TIDA-010961. Then angle of the reference encoder is compared against the inductive encoder angle. The air gap is set to the default value of 0.5mm. A total of 2500 angle samples are collected over one revolution.

Figure 4-17 and Figure 4-18 show the mechanical angular error with offset and gain calibration.

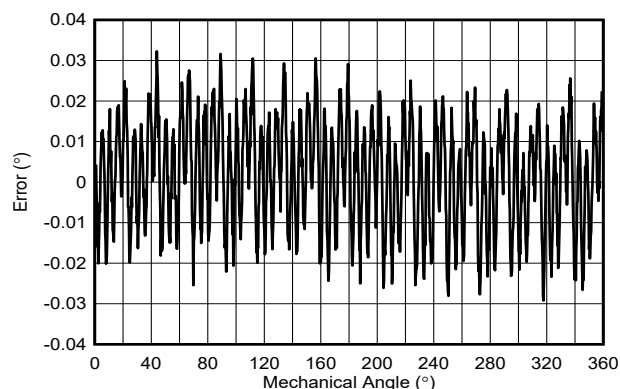


Figure 4-17. Rotary Angle Accuracy Over One Mechanical Cycle With Offset and Gain Calibration at 25°C Ambient

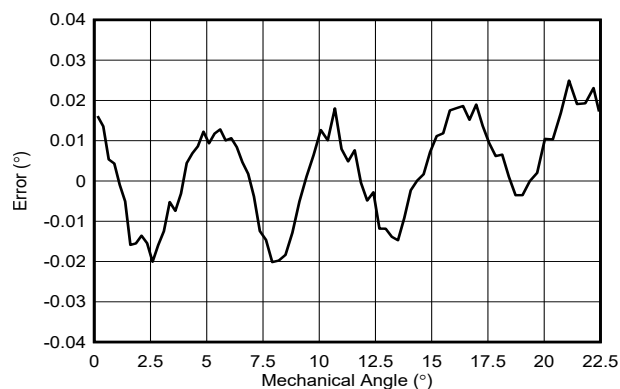


Figure 4-18. Rotary Angle Accuracy Over One Electrical Cycle With Offset and Gain Calibration at 25°C Ambient

For the repeatability test, the angle data is collected twice with the same calibration parameter. Figure 4-19 shows error results of two cycles with calibration. The data of cycle 1 and cycle 2 almost completely overlap, this means there is reliable repeatability of TIDA-010961.

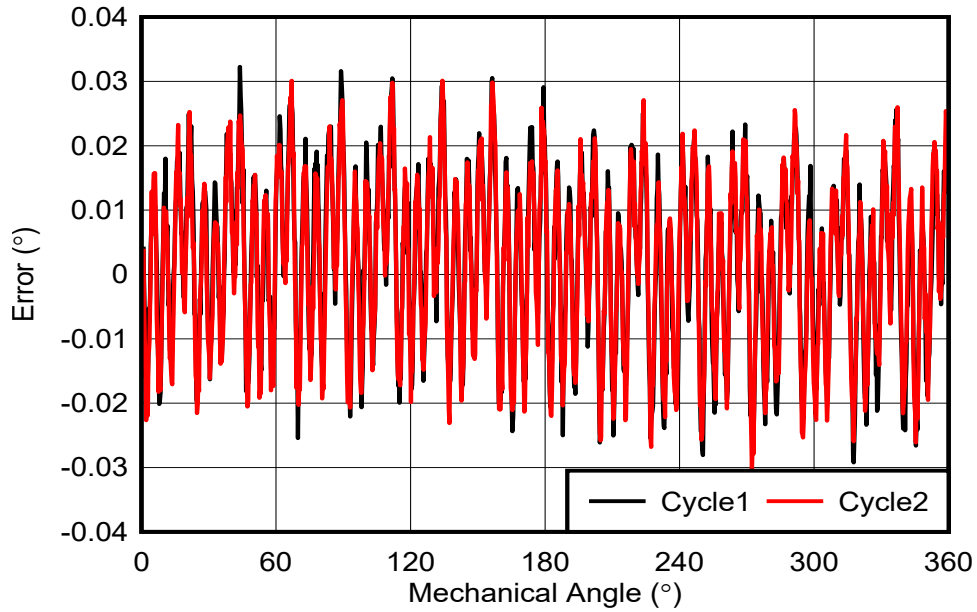


Figure 4-19. Rotary Angle Accuracy With Offset and Gain Calibration at 25°C Ambient, Repeated Test Run

4.4.4 Impact of Air Gap on Noise, 4th Electrical Harmonics and Total Angle Accuracy

With the air gap increasing, the electromagnetic field generated by excitation coils reduces and leads to higher LDC5072 noise. This section analyzes the influence of the air gap on TIDA-010961. By using different motor shaft adapters, the air gap changes from 0.5mm to 1.2mm. Repeat the test procedure described in section. [Figure 4-20](#) to [Figure 4-25](#) show the test results.

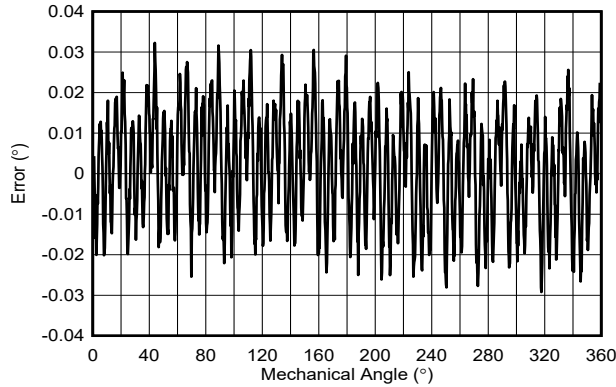


Figure 4-20. Rotary Angle Accuracy Over One Mechanical Cycle at 0.5mm Air Gap

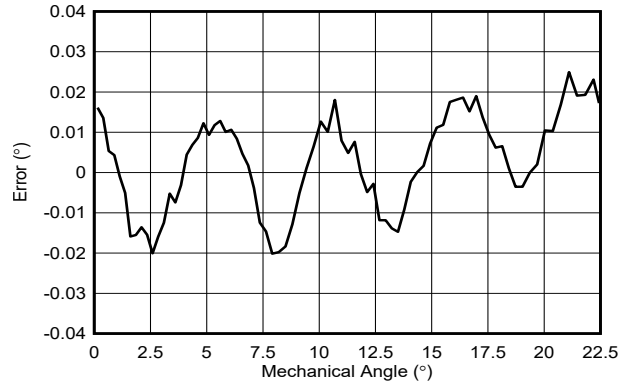


Figure 4-21. Rotary Angle Accuracy Over One Electrical Cycle at 0.5mm Air Gap

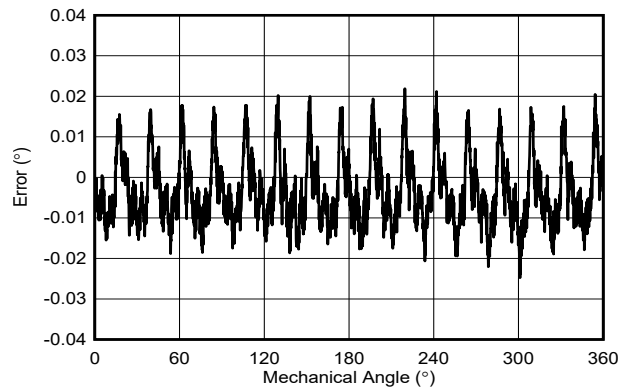


Figure 4-22. Rotary Angle Accuracy Over One Mechanical Cycle at 0.8mm Air Gap

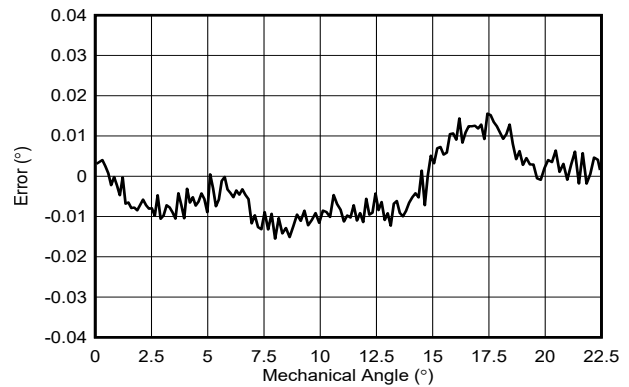


Figure 4-23. Rotary Angle Accuracy Over One Electrical Cycle at 0.8mm Air Gap

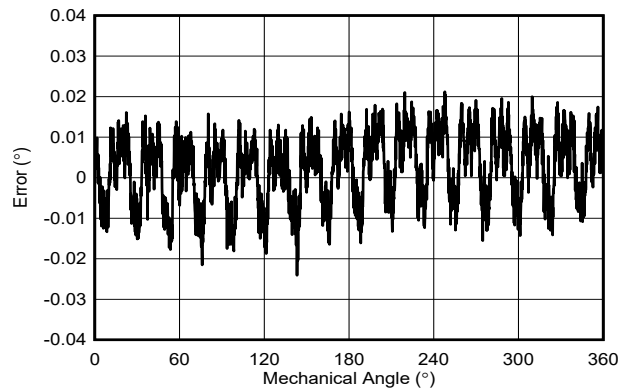


Figure 4-24. Rotary Angle Accuracy Over One Mechanical Cycle at 1.2mm Air Gap

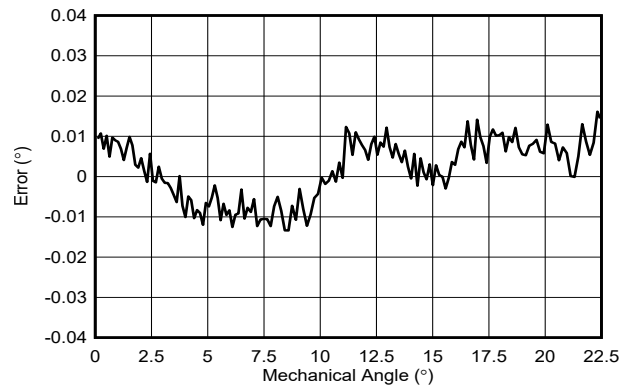


Figure 4-25. Rotary Angle Accuracy Over One Electrical Cycle at 1.2mm Air Gap

Under different air gaps, the angle error are all below ± 0.04 degrees. Besides, the rotary angle accuracy over one electrical cycle figure shows the harmonics vary with air gap changes.

FFT analysis is used to further analyze the air-gap influence on harmonics. Table 4-7 shows the results. At a lower air gap, the 4th harmonic is larger. But as air gap increases, the static noise goes higher and the 4th harmonic error decreases. There is a tradeoff between encoder resolution and encoder accuracy.

Table 4-7. Harmonic in Electrical Angle

AIR GAP	STATIC NOISE (DEG) ⁽¹⁾	1 ST HARMONIC (DEG) ⁽²⁾	2 ND HARMONIC (DEG) ⁽²⁾	4 TH HARMONIC (DEG) ⁽²⁾
0.5mm	0.0015	0.0068	0.0043	0.0110
0.8mm	0.0023	0.0085	0.0042	0.0039
1.2mm	0.0025	0.0080	0.0045	0.0038

(1) All data are 1-sigma RMS value

(2) The harmonic order is referred to electrical cycle

4.4.5 Power Consumption Measurement

Connect the encoder with a 12V supply, record the current consumption of the whole encoder.

The current consumption under 12V power supply is 39mA. This value includes both the consumption of the coil and the consumption of all signal chain chips. Resolver has similar working principles with inductive encoder which also needs to inject an excitation signal, but resolver typically needs higher excitation current from 40mA to 200mA. Inductive encoder has significant advantages on power consumption compared with resolver.

5 Design and Documentation Support

5.1 Design Files

5.1.1 Schematics

To download the schematics, see the design files at [TIDA-010961](#).

5.1.2 BOM

To download the bill of materials, see the design files at [TIDA-010961](#).

5.1.3 PCB Layout

To download the PCB layout, see the design files at [TIDA-010961](#).

5.1.4 Altium Project Files

To download the Altium Designer® files, see the design files at [TIDA-010961](#).

5.1.5 Gerber Files

To download the Gerber files, see the design files at [TIDA-010961](#).

5.1.6 Assembly Drawings

To download the Assembly Drawings, see the design files at [TIDA-010961](#).

5.2 Tools and Software

[LDC507x Sensor Design Tool](#)

The LDC5072X design tool is a powerful resource to accelerate the design and implementation of inductive PCB sensors for monitoring motor position with the LDC5072-Q1.

[MSPM0-SDK](#)

The MSPM0 SDK provides the ultimate collection of software, tools and documentation to accelerate the development of applications for the MSPM0 MCU platform under a single software package.

5.3 Documentation Support

1. Texas Instruments, [Choosing a position sensor in motor control Analog Design Journal](#)
2. Texas Instruments, [Calibration of AMR Angle Sensors Application Report](#)
3. Texas Instruments, [Achieving Highest System Angle Sensing Accuracy Application Note](#)
4. Texas Instruments, [High-resolution, low-latency, compact absolute angle encoder reference design with AMR sensor reference design](#)
5. Texas Instruments, [48V, 85A small form-factor three-phase inverter reference design for integrated motor drives reference design](#)
6. Texas Instruments, [TMS320F28003x Real-Time Microcontrollers Technical Reference Manual Technical Reference Manual](#)

5.4 Support Resources

[TI E2E™ support forums](#) are an engineer's go-to source for fast, verified answers and design help — straight from the experts. Search existing answers or ask your own question to get the quick design help you need.

Linked content is provided "AS IS" by the respective contributors. They do not constitute TI specifications and do not necessarily reflect TI's views; see TI's [Terms of Use](#).

Trademarks

TI E2E™ and LaunchPad™ are trademarks of Texas Instruments.

Arm® and Cortex® are registered trademarks of ARM Limited.

are registered trademarks of Arm Limited.

Altium Designer® is a registered trademark of Altium LLC.

All trademarks are the property of their respective owners.

6 About the Author

YUFENG ZHANG is a system engineer in the Industrial Systems Motor Drive team at Texas Instruments, where he is responsible for specifying and developing custom drive components and assemblies for industrial applications.

MARTIN STAEBLER is Senior Member Technical Staff in the Industrial Systems Motor Drive team at Texas Instruments, where he is responsible for specifying and developing custom drive components and assemblies for industrial applications.

IMPORTANT NOTICE AND DISCLAIMER

TI PROVIDES TECHNICAL AND RELIABILITY DATA (INCLUDING DATA SHEETS), DESIGN RESOURCES (INCLUDING REFERENCE DESIGNS), APPLICATION OR OTHER DESIGN ADVICE, WEB TOOLS, SAFETY INFORMATION, AND OTHER RESOURCES "AS IS" AND WITH ALL FAULTS, AND DISCLAIMS ALL WARRANTIES, EXPRESS AND IMPLIED, INCLUDING WITHOUT LIMITATION ANY IMPLIED WARRANTIES OF MERCHANTABILITY, FITNESS FOR A PARTICULAR PURPOSE OR NON-INFRINGEMENT OF THIRD PARTY INTELLECTUAL PROPERTY RIGHTS.

These resources are intended for skilled developers designing with TI products. You are solely responsible for (1) selecting the appropriate TI products for your application, (2) designing, validating and testing your application, and (3) ensuring your application meets applicable standards, and any other safety, security, regulatory or other requirements.

These resources are subject to change without notice. TI grants you permission to use these resources only for development of an application that uses the TI products described in the resource. Other reproduction and display of these resources is prohibited. No license is granted to any other TI intellectual property right or to any third party intellectual property right. TI disclaims responsibility for, and you will fully indemnify TI and its representatives against, any claims, damages, costs, losses, and liabilities arising out of your use of these resources.

TI's products are provided subject to [TI's Terms of Sale](#) or other applicable terms available either on [ti.com](https://www.ti.com) or provided in conjunction with such TI products. TI's provision of these resources does not expand or otherwise alter TI's applicable warranties or warranty disclaimers for TI products.

TI objects to and rejects any additional or different terms you may have proposed.

Mailing Address: Texas Instruments, Post Office Box 655303, Dallas, Texas 75265

Copyright © 2025, Texas Instruments Incorporated